The Plant Journal - Supporting Information

Molecular mechanisms and hormonal regulation underpinning morphological dormancy: a case study using *Apium graveolens* (Apiaceae)[CC-BY]

Matthew Walker[1,2], Marta Pérez[1], Tina Steinbrecher[1], Frances Gawthrop[2], Iva Pavlović[3], Ondřej Novák[3], Danuše Tarkowská[3], Miroslav Strnad[3], Federica Marone[4], Kazumi Nakabayashi[1*] and Gerhard Leubner-Metzger[1,3*]

[1] Department of Biological Sciences, Royal Holloway University of London, Egham, Surrey, TW20 0EX, United Kingdom, Web: 'The Seed Biology Place' - www.seedbiology.eu

[2] Tozer Seeds, Tozer Seeds Ltd, Cobham, Surrey, KT11 3EH, United Kingdom

[3] Laboratory of Growth Regulators, Institute of Experimental Botany, Czech Academy of Sciences and Faculty of Science, Palacký University Olomouc, CZ-78371 Olomouc, Czech Republic

[4] Swiss Light Source, Paul Scherrer Institute, CH-5232 Villigen, Switzerland

* For correspondence to gerhard.leubner@rhul.ac.uk and kazumi.nakabayashi@rhul.ac.uk (shared corresponding authors)

Detail Experimental Procedures and Notes

Analysis of dormancy classes across Apiaceae phylogeny

The Apiaceae is an advanced Asterid family with ca. 430 genera divided into the four subfamilies Apioideae, Saniculoideae, Azorelloideae, and Mackinlayoideae, which are considered to be monophyletic groupings (Vandelook *et al.*, 2012, Calvino *et al.*, 2016, Wen *et al.*, 2020). The Apiaceae phylogenies of Calvino et al. (2016) and Vandelook et al. (2012) were based on ribosomal ITS and rps16 sequences from a large number of accessions (211 and 323, respectively), and the most recent phylogeny of Wen et al. (2020) was based on 3351 single copy gene trees. To generate the phylogeny presented in Figure 1 we reduced the species level phylogenies of Calvino et al. (2016) and Vandelook et al. (2012) to tribe or clade level and used as divergence times of the nodes the point estimate of divergence times values from Table 1 in Calvino et al. (2016). Fossil calibration of their Apiaceae phylogenies resulted in similar estimated divergence times (Calvino *et al.*, 2016, Wen *et al.*, 2020). The genus level phylogeny of the Apieae tribe (Figure 1) was also generated from the species level phylogenies of Calvino et al. (2016) and Vandelook et al. (2012) by combining them and reducing them to genus level. The phylogenetic relationships between the Apieae genera (Figure 1) are in agreement with detail analysis of this tribe and the Apioideae subfamily (Spalik *et al.*, 2010, Vandelook *et al.*, 2012, Jimenez-Mejias and Vargas, 2015, Calvino *et al.*, 2016, Wen *et al.*, 2020). According to Li at al. (2019) the origin of the Apiales with its families Apiaceae, Araliaceae, Myodocarpaceae, Pittosporaceae, Griseliniaceae and Pennantiaceae was in the Late Cretaceous with a median estimated node age of 80.5 MYA. The estimated origin of the Apiaceae as the youngest Apiales family was in the Late Cretaceous: 51.9 MYA (median estimated node age, Li *et al.*, 2019), 65.8 MYA (point estimate crown age, Calvino *et al.*, 2016) and 64.3 MYA (estimated age stem group, Vandelook *et al.*, 2012). For the large Apioideae subfamily the estimated divergence times were 58.4 MYA (Calvino *et al.*, 2016), 56.7 MYA (Wen *et al.*, 2020) and 59.3 MYA (Vandelook *et al.*, 2012).

This solid phylogeny of the Apiaceae with its four monophyletic subfamilies Apioideae, Saniculoideae, Azorelloideae and Mackinlayoideae (Vandelook *et al.*, 2012, Calvino *et al.*, 2016, Wen *et al.*, 2020) allowed us to investigate the family-wide distribution of the morphophysiological (MD) and morphophysiological (MPD) seed dormancy classes on tribe, clade, genus (Figure 1) and species (SI Data S1) level. In order to do this, we accessed the Baskin Dormancy Database (http://www.charlesgwillis.com/baskins-dormancy-database, accessed 29/11/2020) which contains the information of the book "Seeds" (Baskin and Baskin, 2014). We extracted the seed dormancy information for the Apiaceae and compiled it in SI Data 1. We then added to the dormancy class (which was either MD or MPD) information the dormancy level and embryo type (Martin, 1946, Baskin and Baskin, 2014). For several species we verified the dormancy class assignment in the original literature cited in the book "Seeds" (Baskin and Baskin, 2014); by doing so we for example found that there is no evidence for *Bunium persicum* to have PD (Baskin and Baskin, 2014) in the cited publication of Sharma and Sharma (2010), but the described MPD was confirmed (Sharifi and Pouresmael, 2006). Further to this, we complemented the 169 entries from the database by 32 new entries for which the dormancy class information was derived from the following literature: *Aciphyllya glacialis* (Hoyle *et al.*, 2014), *Ammi majus* (Madakadze *et al.*, 1993, Jimenez-Mejias and Vargas, 2015), *Anethum graveolens* (Unver and Tilki, 2012, Jimenez-Mejias and Vargas, 2015), *Angelica keiskei* (Zhang *et al.*, 2019), *Apium bermejoi* (Cursach and Rita, 2012b), *Apium graveolens*

(Jacobsen *et al.*, 1976, Jacobsen and Pressman, 1979, Van der Toorn and Karssen, 1992), *Bupleurum aureum* (Baskin and Baskin, 2014, Chugunov and Khapugin, 2020), *Bifora radicans* (Mennan, 2003), *Bubon macedonicum* (Di Cecco *et al.*, 2018), *Cenolophium denudatum* (Baskin and Baskin, 2014), *Cicuta virosa* (Cho *et al.*, 2018), *Conium maculatum* (Baskin and Baskin, 1990), *Conopodium majus* (Blandino *et al.*, 2019), *Cuminum cyminum* (Soltani *et al.*, 2019), *Deverra triradiata* (Bhatt *et al.*, 2019, Bhatt *et al.*, 2020), *Eryngium sparganophyllum* (Wolkis *et al.*, 2020), *Eryngium viviparum* (Ayuso *et al.*, 2017), *Ferula ovina* (Fasih and Afshari, 2017), *Hladnikia pastinacifolia* (Sajna *et al.*, 2019), *Heracleum asperum* (Baskin and Baskin, 2014), *Heracleum laciniatum* (Baskin and Baskin, 2014), *Heracleum sosnowskyi* (Baskin and Baskin, 2014, Koryzniene *et al.*, 2019), *Heracleum sphondylium* (Baskin and Baskin, 2014), *Naufraga balerrica* (Ronse *et al.*, 2010, Cursach and Rita, 2012a, Jimenez-Mejias and Vargas, 2015), *Osmorhiza claytonia* (Hawkins *et al.*, 2007), *Petagnaea gussonei* (De Castro *et al.*, 2015), *Petroselium crispum* (Olszewski *et al.*, 2004, Olszewski *et al.*, 2005, Jimenez-Mejias and Vargas, 2015), *Peucedanum ostruthium* (Baskin and Baskin, 2014), *Pimpinella anisum* (Lamichaney *et al.*, 2016), *Rouya polygama* (Santo *et al.*, 2014), *Sison amomum* (Van Assehe *et al.*, 2011), and *Turgenia latifolia* (Nurulla *et al.*, 2014).

The Apiaceae also provide many examples that individual species, populations and even individual plants can produce mixtures of MD (small embryo, no physiological dormancy) and MPD (small embryo, physiological dormancy) diaspores, as well as mixtures of diaspores with different levels of MPD (Figure 1, Data S1). This is consistent with ecophysiological studies indeed suggest that there is a very close association between the MD and MPD classes, as well as the MPD levels (Baskin and Baskin, 2014). Examples for species with both MD and MPD fruits either on the same plant or on plants from distinct populations or depending on the season or year are found in all Apiaceae tribes (labelled with "*" in Figure 1 and Data S1) and include *Cicuta maculate*, *Conium maculatum*, *Conopodium majus*, *Pastinaca sativa*, *Ptilimnium nuttallii*, *Smyrnium olusatrum*, *Torilis arvensis*, *Trepocarpus aethusae* (Sorensen and Holden, 1974, Baskin and Baskin, 1975, Baskin and Baskin, 1979, Grime *et al.*, 1981, Mulligan and Munro, 1981, Baskin and Baskin, 1990, Baskin and Baskin, 2014, Blandino *et al.*, 2019). Similarly, there are examples for mixtures of different MPD levels in Apiaceae diaspore collections from one species (Data S1). The dormancy of *Ferula gummosa* was initially described deep complex MPD (Baskin and Baskin, 2014). Subsequent work by Zardari et al. (2019) demonstrated for a *F. gummosa* seed lot that 80% of the seeds had indeed deep complex MPD, but the other 20% had intermediate complex MPD. The presence of both intermediate and deep complex MPD was interpreted as adaptation to its natural habitat (Zardari *et al.*, 2019). Work with *Sanicula* species demonstrated that they have either non-deep complex or deep complex MPD, and *Sanicula canadensis* can have both non-deep complex and deep complex MPD (Data 1, Vandelook and Van Assche, 2008, Hawkins *et al.*, 2010, Baskin and Baskin, 2014). Taken together, the associations between MD and the different levels of MPD are evident across the Apiaceae and provide a multitude of related model systems to study the adaptations of diaspores with underdeveloped embryos in one family.

Synchrotron-Based X-Ray Tomographic Microscopy (SXRTM)

Celery seeds were sampled in the dry state as well as after 5 days of imbibition in water. Samples were fixed, critical point dried and mounted to 3 mm diameter brass pins using the method described by Arshad *et al.* (2020). SXRTM was performed using the TOmographic Microscopy and Coherent rAdiology experimenTs (TOMCAT) beamline at the Swiss Light Source, Paul Scherrer Institute,

Villigen, Switzerland (Project ID: 20180809). Data were acquired using the 10x objective and a sCMOS camera (PCO.edge; PCO, Kelheim, Germany) with an exposure time of 80 ms at 12keV and a voxel size of 0.65 μm. Projections were post-processed (Paganin phase retrieval) and reconstructed using a Fourier-based algorithm (Marone and Stampanoni, 2012). Subsequently images were reconstructed and processed using Avizo™ 9.5.0 (Thermofisher Scientific™, Visualization Science Group Inc., Burlington, MA, USA) as described (Arshad *et al.*, 2020).

Phytohormone Quantification

Gibberellins. The sample preparation and analysis of GAs was performed according to the method described (Urbanova *et al.*, 2013) with some modifications described here. Briefly, aliquots of 10 mg of lyophilized samples were combined with 1 ml of ice-cold extraction solution (80% acetonitrile + 5% formic acid). Samples were homogenised at 27 Hz for 3 min using 2.8-mm zirconium oxide beads (Next Advance Inc., Troy, NY, USA) and an MM400 vibration mill (Retsch Technology GmbH, Haan, Germany), before being sonicated for 5 mins using an ultrasonic bath. Samples were then extracted overnight at 4 °C with rotation using a benchtop laboratory rotator (Bibby Scientific Ltd., Staffordshire, UK) after adding deuterium labelled GA internal standards ($[^2H_2]GA_1$, $[^2H_2]GA_3$, $[^2H_2]GA_4$, $[^2H_2]GA_5$, $[^2H_2]GA_6$, $[^2H_2]GA_7$, $[^2H_2]GA_8$, $[^2H_2]GA_9$, $[^2H_2]GA_{15}$, $[^2H_2]GA_{19}$, $[^2H_2]GA_{20}$, $[^2H_2]GA_{24}$, $[^2H_2]GA_{29}$, $[^2H_2]GA_{34}$, $[^2H_2]GA_{44}$, $[^2H_2]GA_{51}$ and $[^2H_2]GA_{53}$; OlchemIm, Czech Republic). The homogenates were centrifuged at 36670 g and 4 °C for 10 min, corresponding supernatants were further purified using reversed-phase and mixed mode SPE cartridges (Waters, Milford, MA, USA) and analysed by ultra-high performance liquid chromatography-tandem mass spectrometry (UHPLC-MS/MS; Micromass, Manchester, UK).

Abscisates and auxins. For quantification of *cis*-S(+)-abscisic acid (ABA), indole-3-acetic acid (IAA) and their metabolites, internal standards, containing 10 pM of $[^2D_6]$-ABA and 5 pM each of $[^2D_3]$-PA, $[^2D_3]$-DPA, $[^{13}C_6]$-IAA, $[^{13}C_6]$-oxIAA, $[^{13}C_6]$-IAAsp and $[^{13}C_6]$-IAAGlu, and 1 ml of ice-cold methanol:water (10:90, v/v) were added to 10 mg of freeze-dried and homogenized sample. Sample mixtures were homogenized using an MM301 Vibration Mill for 5 min at 27 Hz (Retsch Technology GmbH), sonicated for 3 min at 4 °C using an ultrasonicator bath, then extracted for 30 min (15 rpm) at 4 °C using a rotary disk shaker. Samples were centrifuged at 20,000 rpm (15 min, 4 °C), the supernatant purified using pre-equilibrated Oasis HLB cartridges (1 cc, 30 mg, Waters), and evaporated to dryness under nitrogen (30 °C) (Flokova *et al.*, 2014). The evaporated samples were reconstituted in 40 μl of the mobile phase (15% acetonitrile, v/v) and analysed by UHPLC-ESI-MS/MS as described by Šimura *et al.* (2018).

All phytohormones were detected using multiple-reaction monitoring mode of the transition of the precursor ion to the appropriate product ion. Masslynx 4.1 software (Waters, Milford, MA, USA) was used to analyze the data and the standard isotope dilution method (Rittenberg and Foster, 1940) was used to quantify the phytohormone levels. Five independent biological replicates were performed.

Quantitative Real-Time RT-PCR (RT-qPCR)

Total RNA extraction and RT-qPCR were as described by Graeber et al. (2011) with the following modifications: Total RNA was extracted using the RNAqueous RNA Isolation kit with addition of the Plant RNA Isolation Aid (Ambion, Austin, Texas, USA). Total RNA was treated with RNase-free DNase (Qiagen, Hilden, Germany) to remove genomic DNA contamination as described (Graeber

et al., 2011). RNA quality and concentration were assessed using a bioanalyzer (Agilent, Santa Clara, California, USA). Synthesis of cDNA was performed using 1 µg total RNA, random hexamers and the Superscript® III synthesis system according to the manufacturer's instructions (Invitrogen, Carlsbad, California, USA). Synthesised cDNA was used for RT-qPCR using ABsolute qPCR SYBR Green Mix (Thermo Fisher Scientific, Waltham, Massachusetts, USA) and a BioRad CFX96 thermal cycler (BioRad, Hercules, California, USA). Primers were designed using Geneious (Geneious, Auckland, NZ) on celery sequences selected through BLASTs of known *Arabidopsis thaliana* and *Nicotiana* spp. sequences on the celery genomic database (Feng *et al.*, 2018). The sequences of all primers can be found in Table S2. PCR products were sanger sequenced to confirm target amplification. Raw fluorescence data was analysed by PCR miner (http://ewindup.info/miner/). Reference gene suitability was assessed by the geNorm software (https://genorm.cmgg.be/), which identified celery homologs of two established seed reference genes (MAP2B, Clathrin) as the most stable and uniformly expressed across all treatments. Target gene normalization was performed against the geometric mean of the expression levels of these two reference genes as described (Graeber *et al.*, 2011). Celery gene nomenclature is based on a combination of sequence homology and expression profile comparison with putative homologous genes in *Arabidopsis thaliana*.

Arshad, W., Marone, F., Collinson, M.E., Leubner-Metzger, G. & Steinbrecher, T. (2020) Fracture of the dimorphic fruits of *Aethionema arabicum* (Brassicaceae). *Botany*, **98**, 65-75.

Ayuso, M., Ramil-Rego, P., Landin, M., Gallego, P.P. & Barreal, M.E. (2017) Computer-assisted recovery of threatened plants: keys for breaking seed dormancy of *Eryngium viviparum*. *Front Plant Sci*, **8**, 2092.

Baskin, C.C. & Baskin, J.M. (2014) *Seeds - Ecology, biogeography, and evolution of dormancy and germination* San Diego, London: Academic Press.

Baskin, J.M. & Baskin, C.C. (1975) Ecophysiology of seed dormancy and germination in *Torilis japonica* in relation to its life cycle strategy. *Bulletin of the Torrey Botanical Club*, **102**, 67-72.

Baskin, J.M. & Baskin, C.C. (1990) Seed germination ecology of poison hemlock, *Conium maculatum*. *Canadian Journal of Botany,* **68**, 2018-2024.

Baskin, J.M. & Baskin, C.M. (1979) Studies on the autecology and population biology of the weedy monocarpic perennial, *Pastinaca sativa*. *J Ecology*, **67**, 601-610.

Bhatt, A., Bhat, N.R. & Gallacher, D. (2020) Intra-plant inflorescence and seed heterogeneity of *Deverra triradiata* (Apiaceae). *Natl Acad Sci Lett*, **43**, 463-465.

Bhatt, A., Bhat, N.R., Santo, A. & Phartyal, S.S. (2019) Influence of temperature, light and salt on the germination of *Deverra triradiata* seeds. *Seed Sci Technol*, **47**, 25-31.

Blandino, C., Fernandez-Pascual, E., Marin, M., Vernet, A. & Pritchard, H.W. (2019) Seed ecology of the geophyte *Conopodium majus* (Apiaceae), indicator species of ancient woodland understories and oligotrophic meadows. *Plant Biol*, **21**, 487-497.

Calvino, C.I., Teruel, F.E. & Downie, S.R. (2016) The role of the Southern Hemisphere in the evolutionary history of Apiaceae, a mostly north temperate plant family. *J Biogeogr*, **43**, 398-409.

Cho, J.S., Jang, B.K. & Lee, C.H. (2018) Seed dormancy and germination characteristics of the endangered species *Cicuta virosa* L. in South Korea. *Hortic Environ Biote*, **59**, 473-481.

Chugunov, G.G. & Khapugin, A.A. (2020) Population status of *Bupleurum aureum* (Apiaceae), a critically endangered plant species in a region of European Russia. *Ecol Quest*, **31**, 45-56.

Cursach, J. & Rita, J. (2012a) Implications of the reproductive biology of the narrow endemic *Naufraga balearica* (Apiaceae) for its conservation status. *Plant Systematics and Evolution*, **298**, 581-596.

Cursach, J. & Rita, J. (2012b) Reproductive biology and reproductive output assessment in natural and introduced subpopulations of *Apium bermejoi*, a 'critically endangered' endemic plant from Menorca (Western Mediterranean). *Nordic Journal of Botany*, **30**, 754-768.

De Castro, O., Gianguzzi, L., Carucci, F., De Luca, A., Gesuele, R. & Guida, M. (2015) Old sleeping Sicilian beauty: seed germination in the palaeoendemic *Petagnaea gussonei* (Spreng.) Rauschert (Saniculoideae, Apiaceae). *Plant Biol*, **17**, 1095-1098.

Di Cecco, V., Paura, B., Bufano, A., Di Santo, P., Di Martino, L. & Frattaroli, A.R. (2018) Analysis of diaspore morphology and seed germination in *Bubon macedonicum* L., a rare species in Italy. *Plant Biosyst*, **152**, 738-748.

Fasih, M. & Afshari, R.T. (2017) The morphophysiological dormancy of *Ferula ovina* seeds is alleviated by low temperature and hydrogen peroxide. *Seed Sci Res*, **28**, 52-62.

Feng, K., Hou, X.L., Li, M.Y., Jiang, Q., Xu, Z.S., Liu, J.X. & Xiong, A.S. (2018) CeleryDB: a genomic database for celery. *Database-Oxford*, ARTN bay070.

Flokova, K., Tarkowska, D., Miersch, O., Strnad, M., Wasternack, C. & Novak, O. (2014) UHPLC-MS/MS based target profiling of stress-induced phytohormones. *Phytochem*, **105**, 147-157.

Graeber, K., Linkies, A., Wood, A.T. & Leubner-Metzger, G. (2011) A guideline to family-wide comparative state-of-the-art quantitative RT-PCR analysis exemplified with a Brassicaceae cross-species seed germination case study. *Plant Cell*, **23**, 2045-2063.

Grime, J.P., Mason, G., Curtis, A.V., Rodman, J., Band, S.R., Mowforth, M.A.G., Neal, A.M. & Shaw, S. (1981) A comparative study of germination characteristics in a local flora. *J Ecology*, **69**, 1017-1059.

Hawkins, T.S., Baskin, C.C. & Baskin, J.M. (2010) Morphophysiological dormancy in seeds of three eastern North American *Sanicula* species (Apiaceae subf. Saniculoideae): evolutionary implications for dormancy break. *Plant Species Biology*, **25**, 103-113.

Hawkins, T.S., Baskin, J.M. & Baskin, C.C. (2007) Seed morphology, germination phenology, and capacity to form a seed bank in six herbaceous layer Apiaceae species of the Eastern Deciduous Forest. *Castanea*, **72**, 8-14.

Hoyle, G.L., Cordiner, H., Good, R.B. & Nicotra, A.B. (2014) Effects of reduced winter duration on seed dormancy and germination in six populations of the alpine herb *Aciphyllya glacialis* (Apiaceae). *Conserv Physiol*, **2**, ARTN cou015.

Jacobsen, J.V. & Pressman, E. (1979) A structural study of germination in celery (*Apium graveolens* L.) seed with emphasis on endosperm breakdown. *Planta*, **144**, 241-248.

Jacobsen, J.V., Pressman, E. & Pyliotis, N.A. (1976) Gibberellin-induced separation of cells in isolated endosperm of celery seed. *Planta*, **129**, 113-122.

Jimenez-Mejias, P. & Vargas, P. (2015) Taxonomy of the tribe Apieae (Apiaceae) revisited as revealed by molecular phylogenies and morphological characters. *Phytotaxa*, **212**, 57-79.

Koryzniene, D., Jurkoniene, S., Zalnierius, T., Gaveliene, V., Jankovska-Bortkevic, E., Bareikiene, N. & Buda, V. (2019) *Heracleum sosnowskyi* seed development under the effect of exogenous application of GA_3. *PeerJ*, **7**, ARTN e6906.

Lamichaney, A., Jain, S.K. & Sooganna (2016) Influence of umbel position on seed quality of anise (*Pimpinella anisum* L.): a minor seed spice. *Bangl J Bot*, **45**, 1245-1250.

Li, H.T., Yi, T.S., Gao, L.M., Ma, P.F., Zhang, T., Yang, J.B., Gitzendanner, M.A., Fritsch, P.W., Cai, J., Luo, Y., Wang, H., van der Bank, M., Zhang, S.D., Wang, Q.F., Wang, J., Zhang, Z.R., Fu, C.N., Yang, J., Hollingsworth, P.M., Chase, M.W., Soltis, D.E., Soltis, P.S. & Li, D.Z. (2019) Origin of angiosperms and the puzzle of the Jurassic gap. *Nat Plants*, **5**, 461-470.

Madakadze, R., Chirco, E.M. & Khan, A.A. (1993) Seed germination of three flower species following matriconditioning under various environments. *Journal of the American Society for Horticultural Science*, **118**, 330-334.

Marone, F. & Stampanoni, M. (2012) Regridding reconstruction algorithm for real-time tomographic imaging. *J Synchrotron Radiat*, **19**, 1029-1037.

Martin, A.C. (1946) The comparative internal morphology of seeds. *The American Midland Naturalist*, **36**, 513-660.

Mennan, H. (2003) The effects of depth and duration of burial on seasonal germination, dormancy and viability of *Galium aparine* and *Bifora radians* seeds. *J Agron Crop Sci*, **189**, 304-309.

Mulligan, G.A. & Munro, D.B. (1981) The biology of canadian weeds. 48. *Cicuta maculata* L., *C. douglasii* (DC.) Coult. & Rose and *C. virosa* L. *Can J Plant Sci*, **61**, 93-105.

Nurulla, M., Baskin, C.C., Lu, J.J., Tan, D.Y. & Baskin, J.M. (2014) Intermediate morphophysiological dormancy allows for life-cycle diversity in the annual weed, *Turgenia latifolia* (Apiaceae). *Aust J Bot*, **62**, 630-637.

Olszewski, M., Pill, W., Pizzolato, T.D. & Pesek, J. (2005) Priming duration influences anatomy and germination responses of parsley mericarps. *Journal of the American Society for Horticultural Science*, **130**, 754-758.

Olszewski, M.W., Pill, W.G. & Pizzolato, T.D. (2004) Germination and embryo anatomy of osmotically primed parsley schizocarps. *Journal of the American Society for Horticultural Science*, **129**, 876-880.

Rittenberg, D. & Foster, G.L. (1940) A new procedure for quantitative analysis by isotope dilution, with application to the determination of amino acids and fatty acids. *Journal of Biological Chemistry*, **133**, 737-744.

Ronse, A.C., Popper, Z.A., Preston, J.C. & Watson, M.F. (2010) Taxonomic revision of European *Apium* L. s.l.: *Helosciadium* WDJ Koch restored. *Plant Systematics and Evolution*, **287**, 1-17.

Sajna, N., Sipek, M., Sustar-Vozlic, J. & Kaligaric, M. (2019) Germination behavior of the extremely rare *Hladnikia pastinacifolia* Rchb. (Apiaceae) - a Pleistocene in situ survivor. *Acta Bot Croat*, **78**, 107-115.

Santo, A., Mattana, E., Hugot, L., Spinosi, P. & Bacchetta, G. (2014) Seed germination and survival of the endangered psammophilous *Rouya polygama* (Apiaceae) in different light, temperature and NaCl conditions. *Seed Sci Res*, **24**, 331-339.

Sharifi, M. & Pouresmael, M. (2006) Breaking seed dormancy in *Bunium persicum* by stratification and chemical substances. *Asian Journal of Plant Sciences*, **5**, 695-699.

Sharma, R.K. & Sharma, S. (2010) Effect of storage and cold-stratification on seed physiological aspects of *Bunium persicum*: a threatened medicinal herb of trans-Himalaya. *International Journal of Botany*, **6**, 151-156.

Simura, J., Antoniadi, I., Siroka, J., Tarkowska, D., Strnad, M., Ljung, K. & Novak, O. (2018) Plant hormonomics: multiple phytohormone profiling by targeted metabolomics. *Plant Physiology*, **177**, 476-489.

Soltani, E., Mortazavian, S.M.M., Faghihi, S. & Akbari, G.A. (2019) Non-deep simple morphophysiological dormancy in seeds of *Cuminum cyminum* L. *J Appl Res Med Aroma*, **15**.

Sorensen, J.T. & Holden, D.J. (1974) Germination of native prairie forb seeds. *J Range Manage*, **27**, 123-126.

Spalik, K., Piwczynski, M., Danderson, C.A., Kurzyna-Mlynik, R., Bone, T.S. & Downie, S.R. (2010) Amphitropic amphiantarctic disjunctions in Apiaceae subfamily Apioideae. *J Biogeogr*, **37**, 1977-1994.

Unver, M.C. & Tilki, F. (2012) Salinity, germination promoting chemicals, temperature and light effects on seed germination of *Anethum graveolens* L. *Bulg J Agric Sci*, **18**, 1005-1011.

Urbanova, T., Tarkowska, D., Novak, O., Hedden, P. & Strnad, M. (2013) Analysis of gibberellins as free acids by ultra performance liquid chromatography-tandem mass spectrometry. *Talanta*, **112**, 85-94.

Van Assehe, J.A., Cornelissen, D. & Vandelook, F. (2011) Germination ecology of *Sison amomum* (Apiaceae) at the northern edge of its distribution range on the European mainland. *Plant Ecol Evol*, **144**, 321-326.

Van der Toorn, P. & Karssen, C.M. (1992) Analysis of embryo growth in mature fruits of celery (*Apium graveolens*). *Plysiologia Plantarum*, **84**, 593-599.

Vandelook, F., Janssens, S.B. & Probert, R.J. (2012) Relative embryo length as an adaptation to habitat and life cycle in Apiaceae. *New Phytol*, **195**, 479-487.

Vandelook, F. & Van Assche, J.A. (2008) Deep complex morphophysiological dormancy in *Sanicula europaea* (Apiaceae) fits a recurring pattern of dormancy types in genera with an Arcto-Tertiary distribution. *Botany*, **86**, 1370-1377.

Wen, J., Yu, Y., Xie, D.F., Peng, C., Liu, Q., Zhou, S.D. & He, X.J. (2020) A transcriptome-based study on the phylogeny and evolution of the taxonomically controversial subfamily Apioideae (Apiaceae). *Ann Bot*, **125**, 937-953.

Wolkis, D., Blackwell, S. & Villanueva, S.K. (2020) Conservation seed physiology of the cienega endemic, *Eryngium sparganophyllum* (Apiaceae). *Conserv Physiol*, **8**, ARTN coaa017.

Zardari, S., Ghaderi-Far, F., Sadeghipour, H.R., Zeinali, E., Soltani, E. & Baskin, C.C. (2019) Deep and intermediate complex morphophysiological dormancy in seeds of *Ferula gummosa* (Apiaceae). *Plant Species Biology*, **34**, 85-94.

Zhang, K.L., Zhang, Y., Walck, J.L. & Tao, J. (2019) Non-deep simple morphophysiological dormancy in seeds of *Angelica keiskei* (Apiaceae). *Sci Hortic-Amsterdam*, **255**, 202-208.
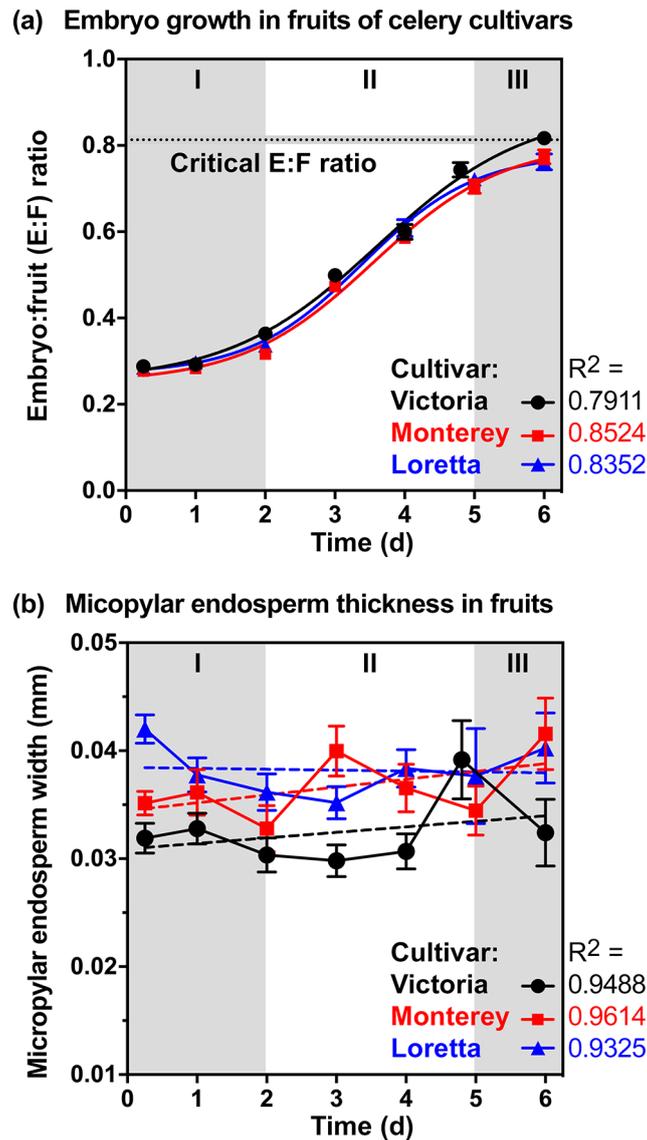
(a) Embryo growth in fruits of celery cultivars

(b) Micopylar endosperm thickness in fruits

Figure S1. Embryo growth and micropylar endosperm thickness in imbibed fruits of three *Apium graveolens* (celery) cultivars. (**a**) Progression of embryo growth inside the fruit and germination during incubation at 20 °C in continuous light. Embryo growth within fruits was scored as embryo:fruit (E:F) ratios calculated from the embryo and fruit lengths. The critical E:F ratio represents the embryo growth threshold value at which radicle protrusion occurs. Mean values ± SEM are presented, N=50. The sigmoidal non-linear regression curve fitted to the E:F ratio data had the indicated goodness of fit R^2 values and P<0.0001. (**b**) Thickness of the micropylar endosperm in imbibed celery fruits. Mean values ± SEM are presented, N=48. Note that linear regression analysis with the R^2 values indicated confirms that the thickness of the micropylar endosperm does not change between the start of imbibition and day 6. Significance was inferred using one-way ANOVA and found to be not significant.
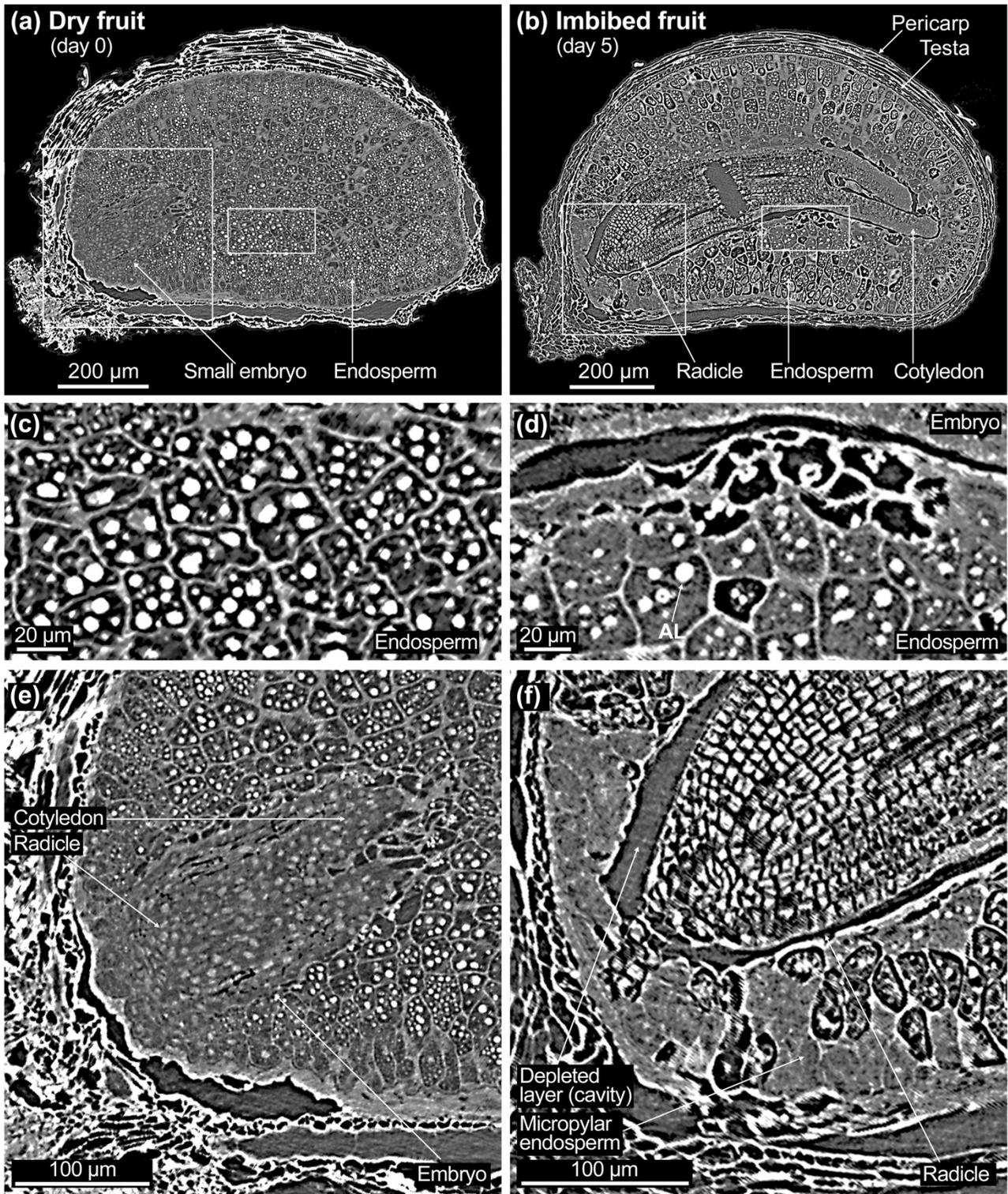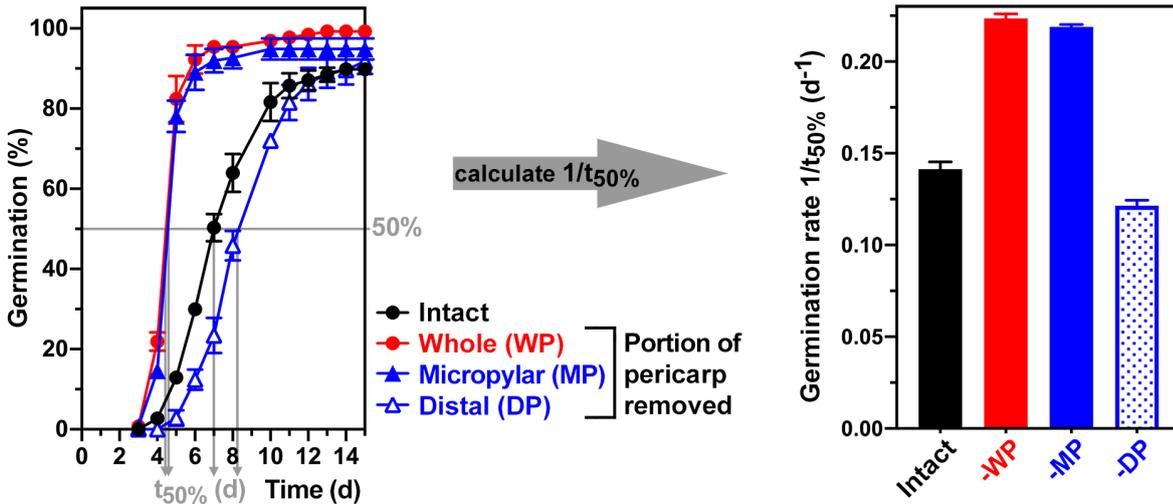
Figure S2. Comparative SXRTM imaging of embryo growth within celery fruits. Digitally produced longitudinal sections of Synchrotron Radiation X-Ray Tomographic Microscopy (SXRTM) images of dry **(a)** and 5-day imbibed fruits **(b)**. White boxes indicate the location of regions amplified in panels c-f. Intact endosperm cells in dry fruits **(c)** compared to degraded endosperm cells adjacent to the growing embryo in 5-day imbibed fruits **(d)**; note the reduction in the number of aleurone grains (AL) and the depleted endosperm cells. **(e)** Small embryo and micropylar endosperm region in dry fruits with dense cells in the radicle and embryonic shoot including the cotyledons. **(f)** Radicle and

micropylar endosperm/pericarp region in 5-day imbibed fruits. The observed radicle tissue pattern as well as the cell size, shape and number, support that the embryo growth occurs by both cell expansion and division, this conclusion is consistent with earlier work (Van der Toorn and Karssen, 1992). The depleted area around the radicle is part of the endospermic cavity which the embryo induces to permit its growth within the fruit. Note further that the expected weakening of the micropylar endosperm during the 5-day imbibition is not associated with a change in the thickness of this tissue (for measurements see Figure S1) and that the micropylar pericarp is a constraint to embryo emergence (see Figure S3).

(a) Effect of pericarp removal on celery fruit germination rate ($1/t_{50\%}$)

(b) Effect of pericarp removal on celery fruit germination uniformity ($t_{75\%}$-$t_{25\%}$)
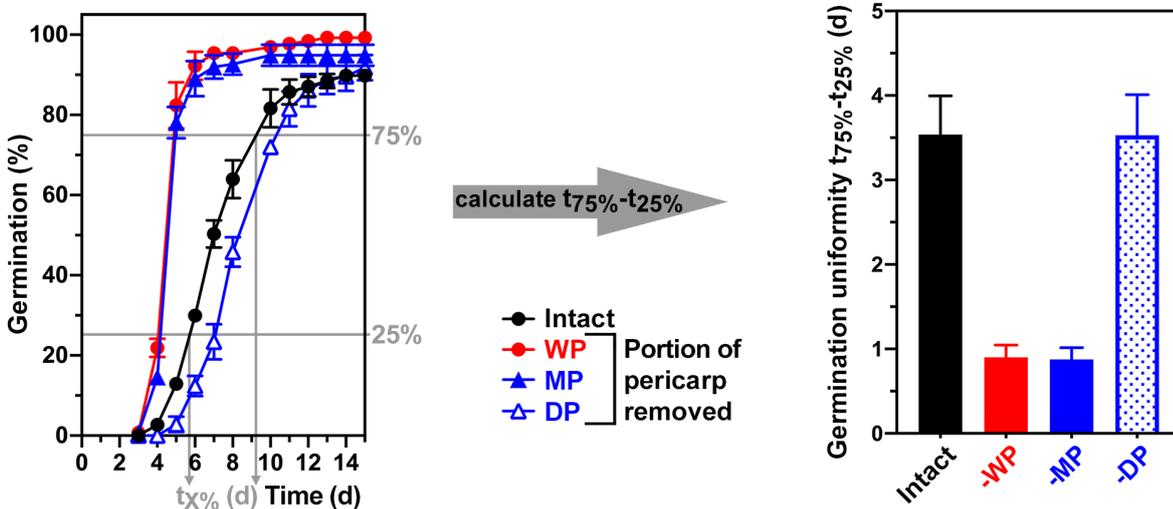

Figure S3. Effect of pericarp removal on celery fruit germination. **(a)** Germination and calculated germination rates ($1/t_{50\%}$) of celery fruits imbibed (20 °C in continuous light) with intact (control) pericarp or with a portion (as indicated) of the pericarp removed. **(b)** Germination and calculated germination uniformity ($t_{25\%}$-$t_{75\%}$) of celery fruits with intact pericarp or with a portion of the pericarp removed. Mean values ± SEM are presented, N=50. Note that removal of the micropylar pericarp, but not the distal pericarp, affected celery fruit germination.

Whole fruit transcript abundances (left y-axis) ●
Compartments (right y-axis): **Embryo** ◆ **Endosperm** ○

(a) GA and ABA-related gene expression (RT-qPCR)

(b) IAA-related gene expression (RT-qPCR)

(c) GA-ABA-regulation of gene expression (RT-qPCR)
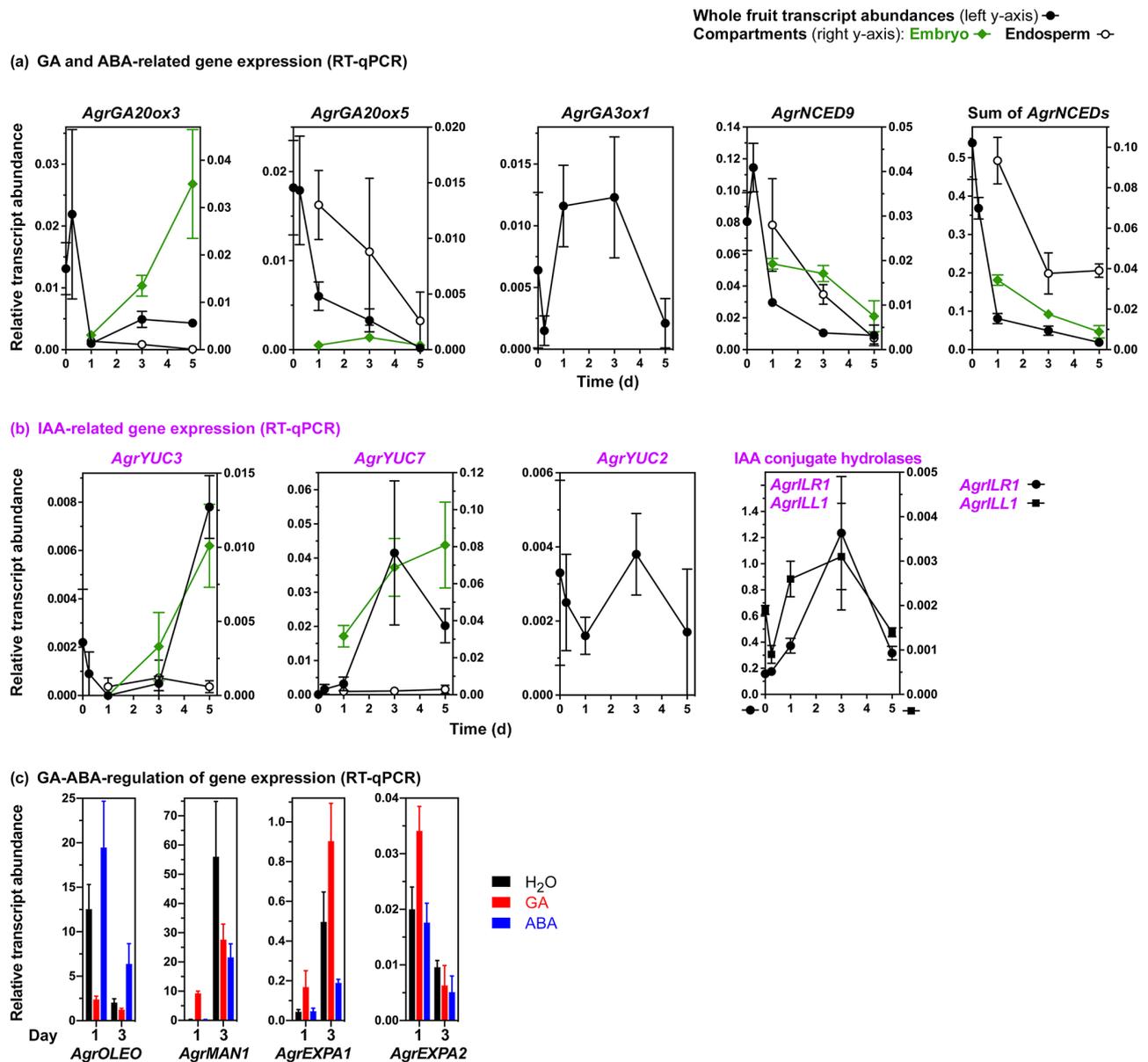

■ H₂O
■ GA
■ ABA

Figure S4. Expression analysis of hormone-related genes during embryo growth and germination of celery fruits. **(a)** Whole fruit and compartment-specific relative transcript abundance patterns (RT-qPCR) during celery fruit imbibition in continuous light at 20 °C of GA- and ABA-related genes. The sum of *AgrNCED* transcripts was calculated from the results obtained for *AgrNCED2*, *ArgNCED6* (Figure 4) and *AgrNCED*9. **(b)** Spatiotemporal expression patterns of IAA-related genes. **(c)** Hormonal regulation of expansin, oleosin and endo-β-1,4-mannanase expression. Mean values ± SEM of 3 (RT-qPCR) biological replicate samples are presented; for further details see Figure 4.
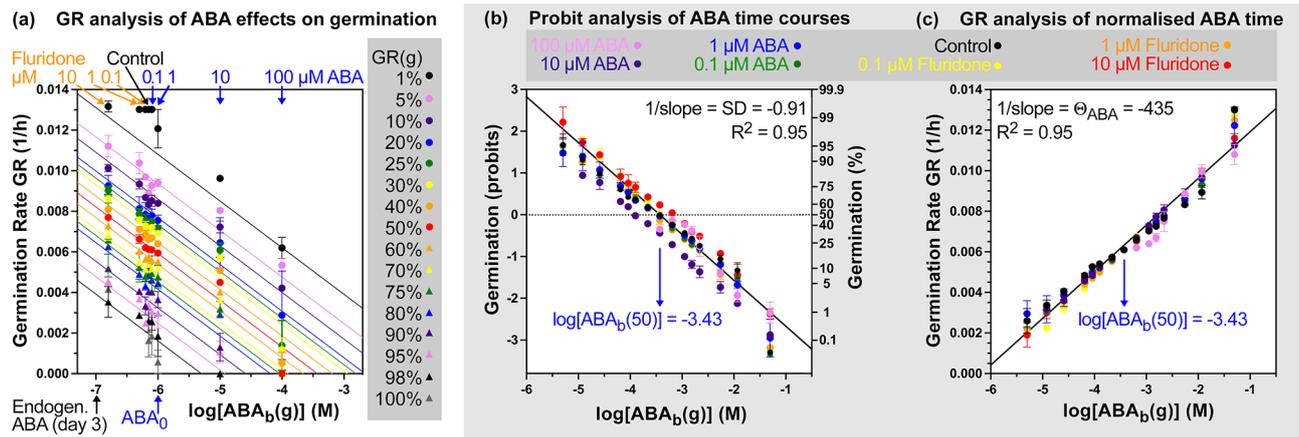
Figure S5. Population-based threshold modelling of ABA effects on celery fruit germination. The theory behind these models is that the sensitivity threshold (or base) values for each hormone are normal distributed within the population and that hormone concentrations above these threshold values trigger dose responses over time which can be described by a hormone time constant (Ni and Bradford, 1992, Bradford and Trewavas, 1994, Fennimore and Foley, 1998, Still and Bradford, 1998, Bradford, 2005, Bradford *et al.*, 2008). **(a)** Germination Rate (GR) analysis of ABA effects on the germination responses of celery fruits. The GR(g) values (speed of germination in 1/hour) are the inverse times to a specified germination percentage g and were derived for the percentages indicated from the obtained time courses (Figure 3b) of the individual germination dishes (each with 50 fruits) for each of the three replicates either without (control) or with ABA or fluridone added at the concentrations indicated. 1 µM ABA (10^{-6} M ABA) was identified as ABA_0, i.e. the highest ABA concentration having no effect on germination. To conduct the mathematical analysis, the 0.1 µM ABA and control which did not appreciably differ from ABA_0, were plotted just adjacent to the 1 µM ABA values (i.e. the 0.1 µM ABA was not plotted at it's 10^{-7} M position). As the next step the obtained slopes and x-axis interceptions were used to derive mean and median values indicative for the parameter of the targeted best-fitting base ABA concentrations ("ABA sensitivity") for each percentage g ($ABA_b(g)$ in log[ABA]), standard deviation SD of mean $log[ABA_b(50)]$, and the ABA time constant Θ_{ABA} (in log[ABA] • h). Repeated Probit analysis (see Figure S5b) and GR analysis of normalised ABA times (see Figure S5c) was conducted starting with the initial and variations of each of the three parameter ($logABA_b(50)$, SD, Θ_{ABA}) until the best fitting values were obtained (R^2 values as indicators). These were then used to plot the lines presented in panel S5a. Responses to the various fluridone concentrations were included and placed at the log[ABA] position where they fit best. Note that for 10 µM fluridone this is for example at -6.8 (0.16 µM ABA) which is very close to the endogenous ABA concentration on day 3 (0.1 µM ABA). These ABA concentrations are well below values which act inhibitory (Figure 4c). **(b)** Repeated probit analysis delivered -3.43 (375 µM ABA) as the best-fitting $log[ABA_b(50)]$ and from the slope of the best regression line ($R^2 = 0.95$) and -0.91 was derived as the best-fitting SD. **(c)** Using these parameter in GR analysis of normalised ABA time delivered Θ_{ABA} = -435 log[ABA] • h as the best estimate for the ABA time constant.

References cited for the hormone modelling:

Bradford, K.J. (2005) Threshold models applied to seed germination ecology. *New Phytologist*, **165**, 338-341.

Bradford, K.J., Benech-Arnold, R.L., Come, D. and Corbineau, F. (2008) Quantifying the sensitivity of barley seed germination to oxygen, abscisic acid, and gibberellin using a population-based threshold model. *J Exptl Bot*, **59**, 335-347.

Bradford, K.J. and Trewavas, J. (1994) Sensitivity thresholds and variable time scales in plant hormone action. *Plant Physiology*, **105**, 1029-1036.

Fennimore, S.A. and Foley, M.E. (1998) Genetic and physiological evidence for the role of gibberellic acid in the germination of dormant *Avena fatua* seeds. *J Exptl Bot*, **49**, 89-94.

Hansen, H. and Grossmann, K. (2000) Auxin-induced ethylene triggers abscisic acid biosynthesis and growth inhibition. *Plant Physiology*, **124**, 1437-1448.

Kucera, B., Cohn, M.A. and Leubner-Metzger, G. (2005) Plant hormone interactions during seed dormancy release and germination. *Seed Sci Res*, **15**, 281-307.

Matilla, A.J. (2020) Seed dormancy: molecular control of its induction and alleviation. *Plants (Basel)*, **9**, 1402.

Ni, B.-R. and Bradford, K.J. (1992) Quantitative models characterizing seed germination responses to abscisic acid and osmoticum. *Plant Physiology*, **98**, 1057-1068.

Still, D.W. and Bradford, K.J. (1998) Using hydrotime and ABA-time models to quantify seed quality of Brassicas during development. *Journal of the American Society for Horticultural Science*, **123**, 692-699.
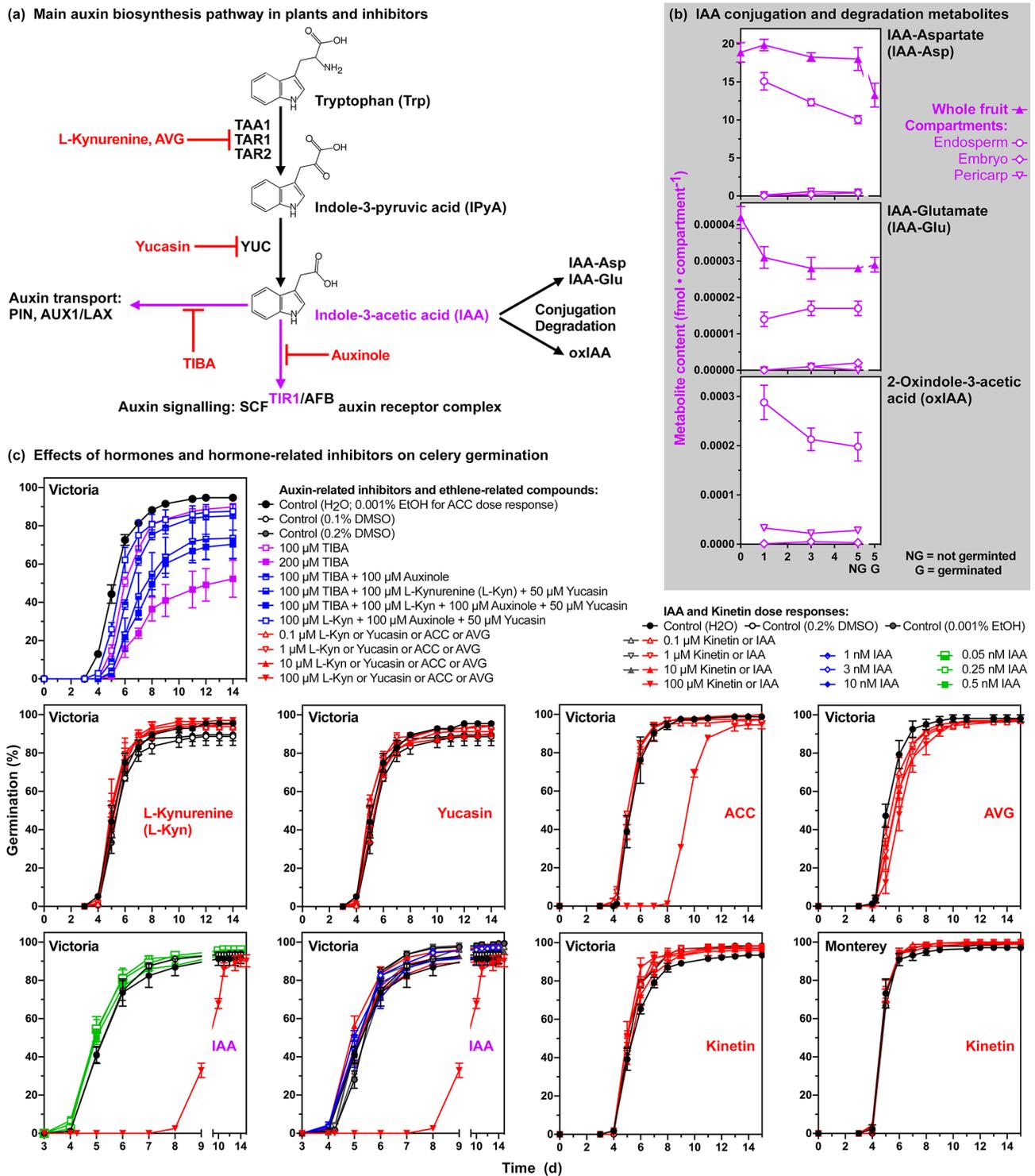
Figure S6. Auxin, cytokinin and ethylene related effects on celery fruit germination. **(a)** Simplified auxin metabolism and signalling with target sites of inhibitors indicated. **(b)** Spatiotemporal metabolite patterns of the major IAA degradation product 2-oxoindole-3-acetic acid (oxIAA) and the conjugated forms IAA-aspartic acid (IAA-Asp) and IAA-glutamate (IAA-Glu). Mean values ± SEM of 5 (metabolites) biological replicate samples are presented; for further details see Figure 5. **(c)** Effects of treatment with hormones and hormone-related 1inhibitors on the germination of celery fruits imbibed at 20 °C in continuous light. Mean values ± SEM of three plates each with 50 fruits are presented. Note that very low IAA concentrations (0.05-0.5 nM) may have a minor promoting effect and that 100 µM IAA significantly delayed celery fruit germination by ca. 4 days. A similar delay was observed with 100 µM of the ethylene precursor 1-aminocyclopropane-1-carboxylic acid (ACC) suggesting that auxin-ethylene may also be involved.

Table S1. Whole celery (*Apium graveolens*) fruit contents of bioactive and inactive gibberellins (GA), abscisic acid (ABA) and associated degradation products, phaseic acid (PA) and dihydrophaseic acid (DPA), indole-3-acetic-acid (IAA) and associated degradation product (oxIAA) and conjugated forms (IAA-Asp and IAA-Glu). Seeds were sampled dry and after 1, 3 or 5 days of incubation in water at 20°C with continuous illumination. For 5-day samples seeds were separated into the non-germinated (NG) and germinated (G) fractions and results shown as indicated. For IAA and ABA seed tissue quantification was performed on fruits separated into the three major compartments (embryo, endosperm, pericarp) at the indicated durations of incubation at 20°C with continuous illumination. The two major GA metabolic pathways, the 13-non-hydroxylated (in blue) and 13-hydroxylated (in red), are indicated. Values are means ± SE of 5 biological replicates and are expressed in pmol/g dry weight for the whole fruit measurements, and fmol/compartment for the segregated tissue analyses, except those metabolites indicated by an asterisk ("*") which are in amol/compartment. <LOD = metabolite was below the limit of detection.

Whole fruits (pmol/g)		Days at 20°C				
		Dry seed	1 day	3 days	5 days (NG)	5 days (G)
Gibberellins (13-non-hydroxylation pathway)	GA_{15}	0.18 ± 0.04	0.08 ± 0.02	0.06 ± 0.01	0.05 ± 0.02	0.09 ± 0.03
	GA_{24}	0.59 ± 0.09	0.25 ± 0.09	0.73 ± 0.07	0.12 ± 0.02	0.25 ± 0.06
	GA_9	0.02 ± 0.00	0.05 ± 0.02	0.09 ± 0.03	0.05 ± 0.02	0.05 ± 0.01
	GA_{51}	16.89 ± 1.35	4.90 ± 0.72	1.97 ± 0.39	3.43 ± 0.23	4.12 ± 0.40
	GA_4	1.18 ± 0.14	0.73 ± 0.11	1.26 ± 0.06	1.35 ± 0.12	1.36 ± 0.11
	GA_{34}	16.14 ± 0.63	3.14 ± 0.08	3.44 ± 0.05	3.77 ± 0.07	3.73 ± 0.21
	GA_{13}	0.51 ± 0.06	0.24 ± 0.04	0.17 ± 0.03	0.18 ± 0.03	0.22 ± 0.02
	GA_7	1.14 ± 0.10	1.08 ± 0.08	1.17 ± 0.12	1.06 ± 0.11	1.13 ± 0.03
Gibberellins (13-hydroxylation pathway)	GA_{53}	3.39 ± 0.46	1.18 ± 0.14	1.68 ± 0.17	1.36 ± 0.14	1.44 ± 0.07
	GA_{44}	4.97 ± 0.33	4.88 ± 0.45	2.52 ± 0.20	4.80 ± 0.29	4.36 ± 0.37
	GA_{19}	25.69 ± 0.58	1.94 ± 0.10	2.12 ± 0.18	2.36 ± 0.11	2.53 ± 0.09
	GA_{20}	15.97 ± 0.77	4.87 ± 0.34	4.95 ± 0.28	5.58 ± 0.14	5.04 ± 0.27
	GA_{29}	373.49 ± 25.9	9.29 ± 0.80	15.84 ± 0.59	21.46 ± 1.06	14.54 ± 0.68
	GA_1	3.94 ± 0.32	1.70 ± 0.19	1.24 ± 0.27	2.02 ± 0.29	2.25 ± 0.28
	GA_8	184.81 ± 7.60	7.97 ± 0.35	7.81 ± 0.35	11.20 ± 1.08	11.79 ± 0.60
	GA_5	0.81 ± 0.14	0.08 ± 0.02	0.05 ± 0.01	0.10 ± 0.02	0.10 ± 0.02
	GA_6	1.02 ± 0.04	0.85 ± 0.02	0.88 ± 0.04	0.81 ± 0.04	0.77 ± 0.02
	GA_3	0.34 ± 0.02	0.08 ± 0.02	0.16 ± 0.03	0.16 ± 0.01	0.11 ± 0.05
Abscisic acid (ABA) and products of its catabolism	ABA	4371.98 ± 241.04	289.90 ± 3.21	172.10 ± 6.77	174.54 ± 11.91	147.84 ± 4.87
	PA	5321.28 ± 540.97	1532.12 ± 201.10	442.88 ± 48.93	403.40 ± 23.76	360.64 ± 38.34
	DPA	233.75 ± 32.55	<LOD	<LOD	<LOD	<LOD
Indole-3-acetic acid (IAA) and catabolic forms (oxIAA, IAA-Asp & IAA-Glu)	IAA	0.86 ± 0.03	0.12 ± 0.01	0.19 ± 0.03	0.21 ± 0.03	0.29 ± 0.03
	oxIAA	0.72 ± 0.05	0.38 ± 0.05	0.36 ± 0.04	0.32 ± 0.03	<LOD
	IAA-Asp	80.58 ± 5.37	97.17 ± 3.67	89.98 ± 2.37	90.50 ± 7.70	64.24 ± 7.07
	IAA-Glu	0.18 ± 0.01	0.15 ± 0.01	0.14 ± 0.01	0.14 ± 0.01	0.14 ± 0.01

Table S1 continued…

Tissue analysis (fmol/compartment, **except those indicated by '*' which are amol/compartment**)			Days at 20°C		
			1 day	**3 days**	**5 days (NG)**
Abscisic acid (ABA) and products of its catabolism	**Embryo**	ABA	4.18 ± 0.09	1.74 ± 0.02	1.90 ± 0.02
		PA	4.35 ± 0.13	2.41 ± 0.16	1.40 ± 0.11
		DPA	1.42 ± 0.20	1.44 ± 0.11	0.76 ± 0.22
	Endosperm	ABA	14.60 ± 0.84	9.09 ± 0.46	9.43 ± 0.19
		PA	568.89 ± 81.02	217.86 ± 35.64	16.24 ± 0.82
		DPA	<LOD	<LOD	<LOD
	Pericarp	ABA	38.15 ± 1.27	28.14 ± 1.09	39.36 ± 0.82
		PA	71.31 ± 5.67	63.81 ± 1.79	107.0 ± 4.34
		DPA	<LOD	<LOD	<LOD
Indole-3-acetic acid (IAA) and catabolic forms (oxIAA, IAA-Asp & IAA-Glu)	**Embryo**	IAA*	0.53 ± 0.13	4.29 ± 0.27	8.02 ± 0.78
		oxIAA*	0.001 ± 0.000	0.005 ± 0.000	0.003 ± 0.000
		IAA-Asp*	45.80 ± 1.93	224.40 ± 12.03	417.40 ± 11.40
		IAA-Glu*	0.001 ± 0.000	0.001 ± 0.000	0.002 ± 0.000
	Endosperm	IAA*	36.14 ± 3.67	27.04 ± 1.87	31.26 ± 2.47
		oxIAA*	0.288 ± 0.035	0.213 ± 0.023	0.198 ± 0.029
		IAA-Asp*	15087.7 ± 1147.5	12308.5 ± 472.9	10032.4 ± 528.4
		IAA-Glu*	0.014 ± 0.002	0.017 ± 0.020	0.017 ± 0.002
	Pericarp	IAA*	11.12 ± 0.52	12.52 ± 0.36	25.80 ± 2.10
		oxIAA*	0.033 ± 0.004	0.022 ± 0.001	0.028 ± 0.001
		IAA-Asp*	125.38 ± 10.06	578.28 ± 18.65	473.90 ± 19.79
		IAA-Glu*	0.000 ± 0.000	0.001 ± 0.000	0.000 ± 0.000

Table S2. Primer sequences used for RT-qPCR.

Gene ID	Forward Primer (5'→3')	Reverse Primer (5'→3')	Amplicon length (bp)[d]
MAP2B[a]	CAGACGAAAATGGAAGAGGGTG	GCATGTGCCCGACATCAAA	125
CLATH[a]	GTTGGCTGGCGTAGAGAAGG	TCCCAGTTACATCACAGCGC	121
GA20ox2[b]	GGTTATGCTAGTAGCTTTACCGGA	TCAACCATAGTGGATGAGGTCTTC	107
GA20ox3[b]	AGCCTTGGTATTGGTCCATCG	GATCCGGTTTCTGGCAAGGA	97
GA20ox5[b]	TTAGGTGTGGAAGCTGAGCAA	TATAGTTATTGCGGTTGGATCAGC	144
GA3ox1[b]	CCAGTTTGTCCGGATCCAGG	CCTTCAATGGGAGGCACACT	146
GA3ox2[b]	AGTCACTGTCAATCGGGAGC	TTCACTCCATGTAACGGCCC	139
GA2ox6[b]	TTTTCGGGTCAATCATTATCCTCC	TGAGGGTCTGAATGTTCTCCAA	141
TAR2[b]	CGCATGGCTGAAATGTGAGG	AAGTGTTTTCCGCCTCTGGT	90
YUC1[b]	CATCAGGCCTTGCAGTCTCA	GGGCAGCTCACAAAAGTTCTG	149
YUC2[b]	GAAAGGCGAGAGTGGGCTAT	CTCTGCCTTCCAACACCGTT	112
YUC3[b]	ATTTTCGCTCGTCGTTGCAC	AGAGGCAATGCAGTCAGCTT	138
YUC7[b]	ACAATGCCTAACTGTCCGGG	AGCATGCATGACATTGCCAC	138
YUC10[b]	AAGAGGAATGGTGCACTGGG	AGGGACCTTCTTGTGGCCT	140
ILL1[b]	GCTATGCAGGAGGAAGTGGA	AATCATGCCGGTGCTCTTGA	130
ILR1[b]	GCAACACAGTGCTCTTGACG	TGTAAACAGGCCTGACCCAG	121
NCED2[b]	GGAAAATCCAGTTGCAGGGC	TCGTCCCAACAAATTCCGGT	87
NCED6[b]	CACCCGTGATCCATGATCCG	CCTCCCAGGCATTCCATAGG	132
NCED9[b]	AGAGGCAGGGATGGTGAACA	ACTTTAGGCCACGGCTCAG	84
CYP707A2[b]	GTTCTGTTCGCGATGAAGCA	AGTGAGCATGAGACACCAGC	124
CYP707A1[b]	TGCCTCCAAAGTCAAGAAGTTTG	CAGCTGCAGGGCTTGAAATC	86
OLEO[b,c]	CACAACACACCAACCACTCC	CGGCGAGGAAAAGTAGGGTT	123
MAN1[b]	GCCGCAGACCCTAGTATGAG	GTGCATTACTACTGCCATCGG	112
EXPA2[b]	ATGGACAGAGATGTGGAGCG	TTGTCATTGGAGAGGGCGTT	127
EXPA1[b]	GAGGTGCTGGAGATGTGCAT	ACTTTGCCAGTTCTGTCCCC	92

[a] Reference gene, [b] Target gene, [c] Primer pair targets several oleosin genes, [d] Amplicon length is based on sequences derived from CeleryDB (http://apiaceae.njau.edu.cn/celerydb).